JOURNAL OF APPLIED ELECTROCHEMISTRY 18 (1988) 499–503

Analysis of primary and secondary current distributions in a wedge-type aluminum–air cell

ROBERT F. SAVINELL

Department of Chemical Engineering, Case Western Reserve University, Cleveland, Ohio 44106, USA

GEORGE G. CHASE

Department of Chemical Engineering, University of Akron, Akron, Ohio 44325, USA

Received 10 April 1986; revised 4 January 1988

The primary and secondary current distributions near the leading edges of the cathode and anode of a wedge-type aluminum–air cell design were analyzed. Numerical calculations were accomplished by using a finite difference method and introducing an overlapping two-grid system technique. The calculations indicate that the current distributions on the cathode and anode at distances from the edges greater than 2 times the cell gap are uniform. In the edge region, the wedge angle between 0 and 10° has a negligible effect on the current distribution. High current densities at the cathode edge, which are detrimental to cathode life, are reduced by kinetic effects and by oversizing the cathode itself. The latter also favors cell performance but adds to the cell costs. An effectiveness factor is introduced which demonstrates the effectiveness of cathode oversize and the sensitivity to kinetics as represented by the Wagner number. The calculations indicate that only marginal performance gains can be expected when the cathode extends beyond the anode a distance greater than that of 1.5 times the anode–cathode gap.

Nomenclature

A1, A2, A3	anode curves 1, 2, 3
b	slope of i vs η curve at mean value of η_{mean} ($A\,cm^{-2}\,V^{-1}$)
C1, C2, C3	cathode curves 1, 2, 3
D	distance between electrodes (cm)
i_s	local current density on electrode ($A\,cm^{-2}$)
I^*	dimensionless local current value defined by Equation 9
N	dimensionless effectiveness factor defined by Equation 10
V_{met}	constant potential of electrode (V)
W	dimensionless Wagner number defined by Equation 7
X	dimensionless cathode oversize defined as x/D
x	position parallel to anode with origin at the anode apex (cm)
y	position perpendicular to electrode surface (cm)
κ	conductivity of electrolyte ($ohm\,cm^{-1}$)
η	surface overpotential (V)
ϕ	potential in solution phase (V)
ϕ_0	potential in solution adjacent to electrode surface (V)

1. Introduction

An aluminum–air power cell has been under development in recent years for possible use in electric vehicles [1, 2]. In this system, the fuel is supplied as solid aluminum which anodically dissolves in a sodium hydroxide solution (or KOH solution). Oxygen from air is reduced at a catalyzed high surface area cathode. The overall reaction can be represented by:

$$Al + 3/2H_2O + 3/4O_2 + NaOH = NaAl(OH)_4$$

The sodium aluminate product is then removed from the cell and sent to a crystallizer where it is decomposed to sodium hydroxide and aluminum trihydroxide. The latter can be recycled as an intermediate feedstock in the aluminum industry.

An essential feature of this power conversion system is that the design of the cell must allow for total consumption and rapid refueling of the aluminum anode. One design given special attention lately is based on a wedge-type geometry [3]. A schematic representation of this design is shown in Fig. 1. This paper reports results of primary and secondary current distribution modeling of this cell design. Of particular interest here is the edge effect where high local current densities can damage the cathode [4]. Several geometrical factors and material properties are considered and implications on cell performance are described.

2. Model and calculation technique

The potential field between the anode and cathode of an electrochemical cell, when concentration gradients

0021-891X/88 $03.00 + .12

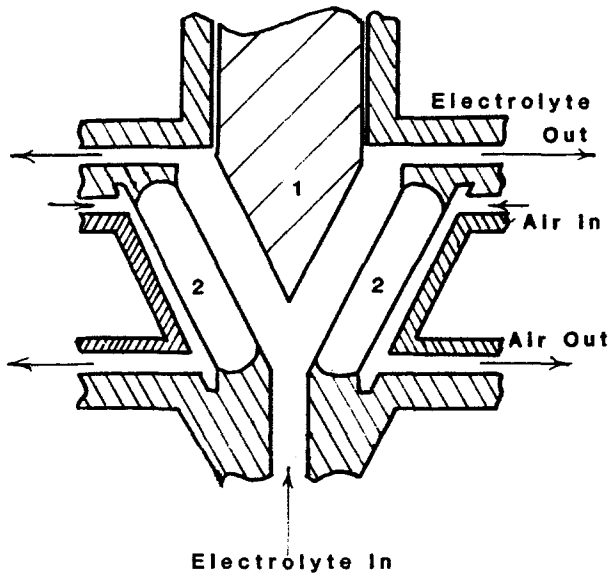

Fig. 1. Schematic representation of the aluminum–air wedge-type cell geometry. In this drawing the angle and the anode thickness are not correctly proportioned to the cell height. In a practical configuration the angle is about 3°, the thickness of the anode entering the cell is about 1.4 cm, the anode–cathode gap is approximately 0.173 cm and the lengths of the anode and cathode are about 11 cm.

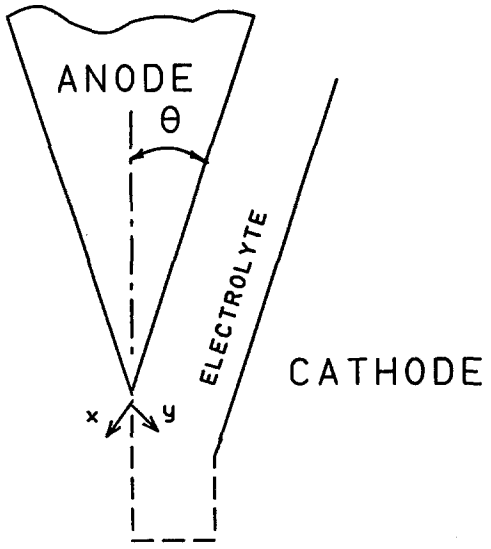

Fig. 2. Section of wedge-type cell under study showing the plane of symmetry.

are not present, is described by the Laplace equation [5]:

$$\nabla^2\phi = 0 \tag{1}$$

In the wedge-cell design, the current and potential distribution lines are uniform except near the wedge apex. This is the region of interest here and is depicted in Fig. 2. In this figure the solid lines represent electrode surfaces while the dashed lines represent either insulating surfaces or planes of symmetry. In this geometry the field is two-dimensional, i.e.

$$\frac{\partial^2\phi}{\partial x^2} + \frac{\partial^2\phi}{\partial y^2} = 0 \tag{2}$$

The boundary conditions of the field include zero potential gradients normal to insulating surfaces and at boundaries far removed from the electrode edges. Two types of electrode boundary conditions were considered. For the primary distribution the anode and cathode potentials were taken to be uniformly constant. In the case of the secondary distribution, the potential at the electrode boundary is modified by a current-dependent surface overpotential, η, or

$$\phi_0 = V_{\text{met}} - \eta(i_s) \tag{3}$$

where V_{met} is constant and i_s is the current density at the electrode surface. In the calculations reported here, the surface overpotential of the anode was ignored and attention was focused only on the cathode kinetic effects.

A linear expression was used to describe the relationship between the current density and the surface overpotential, i.e.

$$i_s = b\eta \tag{4}$$

where b is a polarization parameter, or

$$b = (\mathrm{d}i_s/\mathrm{d}\eta)_{\eta_{\text{mean}}} \tag{5}$$

In the case of Tafel polarization (which is the likely case here), this expression can still be used but V_{met} in Equation 3 is corrected by a constant [6].

The current density at the electrode surface can be expressed as

$$i_s = -\kappa\left(\frac{\mathrm{d}\phi}{\mathrm{d}y}\right)_{\text{electrode surface}} \tag{6}$$

where y represents the direction normal to the electrode surface. The dimensionless Wagner number is introduced which is defined by

$$W = \kappa/(Db) \tag{7}$$

where D is a characteristic dimension, or the gap between the anode and the cathode in this case. The boundary condition given by Equation 3 can now be written as:

$$\phi_0 = V_{\text{met}} + DW\left(\frac{\mathrm{d}\phi}{\mathrm{d}y}\right)_{\text{electrode surface}} \tag{8}$$

The distribution of potential and current can be obtained by solving the Laplace equation subjected to the appropriate boundary conditions. In the case of the primary distribution, simple geometries like the one here can be found by analytical techniques [7]. However, secondary distributions usually require numerical calculation techniques.

A number of numerical approaches are available for solving the Laplace equation. Finite differences [8] and boundary integral [9] methods are two techniques commonly employed in electrochemical analysis. A

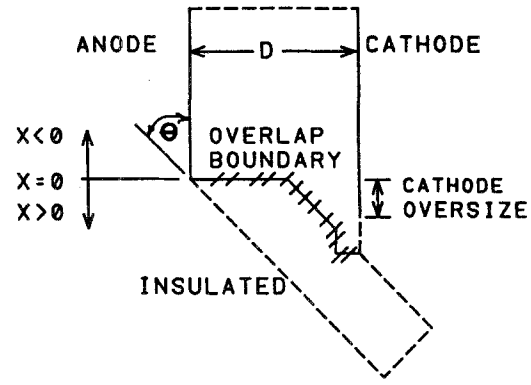

Fig. 3. The overlapping boundary geometry used in numerical calculations.

conceptually simple finite difference Gauss–Seidel iterative procedure [10] was applied here.

An expanded view of the portion of the cell being modeled is shown in Fig. 3. When the cathode terminates at the dimensionless distance of $X = 0$ (where $X = x/D$), the cathode and anode dimensions are equivalent. If the cathode terminates at $X > 0$ then the cathode extends beyond the anode and this is termed 'cathode oversize'.

In the wedge-cell design, when θ is equal to zero and the insulating surfaces are parallel to a grid line of the coordinate system used for the finite difference representation, then the numerical integration is easily accomplished. However, when the insulated surfaces do not conveniently follow a grid line, the programming becomes much more complex and calculations consume significant amounts of computer time before converging. These problems have been experienced here.

In order to accelerate the rate of convergence, the potential field was sectioned using two systems of overlapping grids which differ by an angle of rotation (θ) and a scale factor. The region of overlap is depicted in Fig. 3. With the two-grid system all of the boundaries of the cell fall on a grid line and thus the insulating surfaces are easily modeled.

Each grid system is solved separately used a Gauss–Seidel relaxation iterative procedure. Three sides of each grid system are defined by the cell geometry as either an insulator or an assigned potential boundary. The fourth side, which overlaps with the other grid system, is modeled as having a known potential value as a function of position and requires an exchange of information from the other grid system.

Each point in a grid system is modeled using the second order accurate four point equation obtained from a truncated Taylor series expansion. With this equation, each point is assigned a new value which is the arithmetic average of the surrounding four grid points [10]. When a given point is located next to the overlapping boundary between the two grid systems, then one or more of its four surrounding grid points lie in the other half of the cell geometry.

In general, the overlapping points that lie in the other half of the cell do not coincide with a grid point of the other coordinate system. The value of an overlapping point is estimated by linear interpolation from the four surrounding grid points of the other grid coordinate system.

This overlapping grid technique is not the most accurate technique available but it does provide advantages such as not requiring a great amount of computer memory, the total number of grid nodes required to describe the system is reasonably small and convergence can be reached in a small number of iterations. This approach resulted in convergence of the calculations performed here within reasonable computational times.

3. Results and discussion

In this study, it is assumed that only the cathode contributes secondary current distribution effects (i.e. a non-zero Wagner number). The cathode was treated as a planar electrode having an apparent surface overpotential for modeling purposes. The apparent surface overpotential therefore is a quantity which includes ohmic, concentration and kinetic effects within a complex porous electrode structure. Using data in the literature on oxygen cathode performance [11] the dimensionless Wagner number (based on cathode kinetics about a mean overpotential at $4000\,\mathrm{A\,m^{-2}}$ number) for an aluminum–air cell under development [12] is approximately 0.56 ($\kappa = 0.52\,\mathrm{ohm\,cm^{-1}}$, $D = 0.173\,\mathrm{cm}$, $b = 5.41\,\mathrm{A\,cm^{-2}\,V^{-1}}$). Recently reported data [13] on high performance oxygen cathodes give a value of $b = 24.2\,\mathrm{A\,cm^{-2}\,V^{-1}}$ at $4000\,\mathrm{A\,m^{-2}}$. This value of b gives a Wagner number of 0.12.

The results of our calculations are presented in terms of current distributions as a function of dimensionless position, X. A dimensionless current density is defined as

$$I^* = \frac{\text{current density at } X}{\text{current density at } X = -2} \qquad (9)$$

The current density at $X = -2$ was chosen as a basis because it was observed to be unaffected by the electrodes' edges.

Figure 4 shows the effect of electrode angle on current distribution when there is no cathode oversize and when the cathode Wagner number is 0.2. Similar distributions were calculated for the primary case and for other Wagner numbers. The high current density at the anode apex helps achieve total anode consumption in this cell design. At the electrode edges a slight decrease in current density with increasing angle is noted (not discernable at the cathode in Fig. 4). The magnitude of this effect, however, is negligible compared to effects due to cathode oversize and cathode kinetic polarizations.

A high local current density at the cathode could damage the materials in the cathode [4]. One way to reduce the current density at the cathode edge is to oversize the cathode. Although this could also improve cell performance by lowering the cell resistance, oversizing the cathode could be expensive. Therefore a

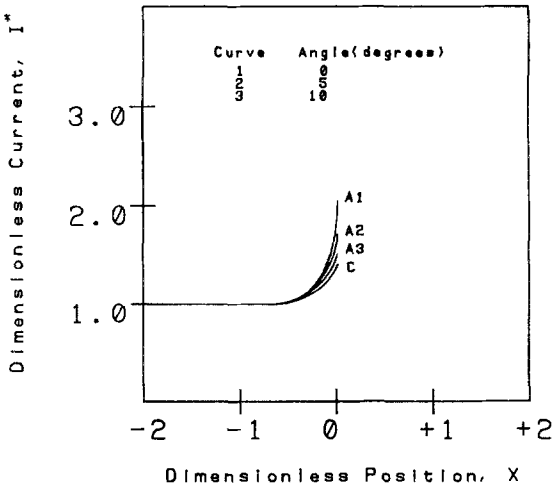

Fig. 4. Current distribution at the anode and the cathode for varying wedge angle. The Wagner number is constant at 0.2 and there is no cathode oversize. Numbers on the labels match the corresponding anode and cathode curves.

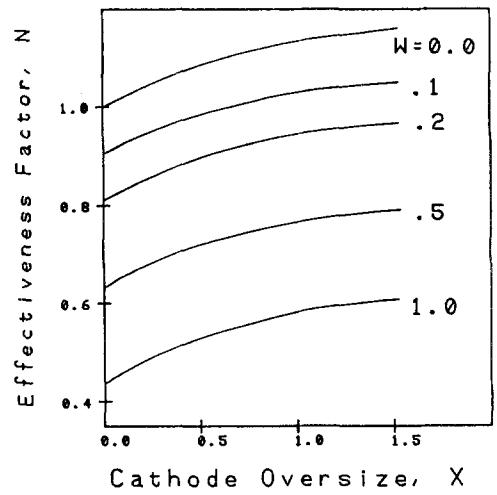

Fig. 6. An effectiveness factor representation for demonstrating the effect of Wagner number and cathode oversize on cell current output.

trade-off must be considered. Figure 5 shows the effect of cathode oversize on the current distribution. Although these results are for a Wagner number of 0.2, similar results are obtained for other Wagner numbers. As shown in Fig. 5, the cathode oversize significantly reduces the cathode edge current density while increasing density at the anode apex which aids total aluminum consumption. However, cathode oversizing in excess of $X = 1$ appear to offer little benefit.

An increasing Wagner number also tends to reduce the locally high current density at the cathode edge. However, increasing the Wagner number by lowering catalytic activity is counterproductive to obtaining good operating performance. The trade-offs involved with cathode oversize and cathode kinetics can be expressed in terms of a design correlation as proposed here:

$$N = I(W, X)/I(0, 0) \qquad (10)$$

The dependent quantity N can be thought of as an 'effectiveness factor' of the leading edge region of the electrodes. This variable represents the cell current output normalized by the output if both the Wagner number and cathode oversize are equal to zero. The independent variable is the cathode oversize and the Wagner number is a design parameter. The correlation based on the numerical calculations of this study is shown in Fig. 6. The curves demonstrate the influence of the Wagner number on the effectiveness factor, which is significantly reduced with increasing values of Wagner number. The effectiveness factors in Fig. 6 increase with cathode oversize because the cell resistance decreases. This effect here is amplified because only the leading edge of the cell is included. However, the figure still demonstrates that the effectiveness factor tends to approach a limiting value when the cathode oversize exceeds a value of 1.5. Therefore, it is apparent that oversizing in excess of $X = 1.5$ does not benefit cell performance.

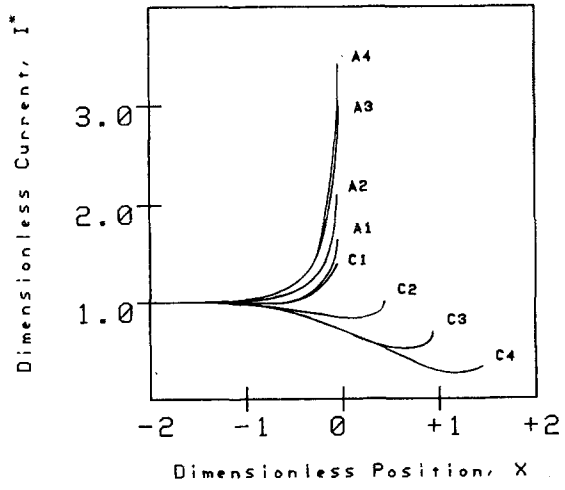

Fig. 5. The effect of cathode oversize on current distribution at the anode and the cathode. The Wagner number is constant at 0.2. Numbers in the legend match the corresponding anode and cathode curves.

4. Conclusions

This study leads to several conclusions regarding the wedge-type cell design for an aluminum–air energy delivery device. Although the angle of the anode taper has little influence on the current distribution near the electrode edges, the cell design still provides for effective total consumption of the aluminum anode. It was shown that by extending the length of the cathode past the edge of the anode (cathode oversize), the locally high edge current distributions on the cathode, which are detrimental to catalyst activity, can be reduced. An additional benefit of cathode oversize is a slightly lower cell resistance, but a disadvantage is higher cost. Increasing the cathode size relative to the anode by more than 1–1.5 times the anode–cathode gap was found to contribute little additional benefit.

This study introduced a method of applying two-grid structures with overlapping boundaries so that electrode and insulating boundaries of non-rectangular geometries of straight sides fall on grid nodes. This method was found to be easy to implement and resulted

in fast convergence in solving the finite difference representation of the Laplace equation.

Acknowledgements

This work was supported by ELTECH Systems Corporation under contract with the United States Lawrence Livermore National Laboratory.

References

[1] J. F. Cooper, Electric & Hydric Vehicle Systems Assessment Seminar, Gainesville, Fl, 12–15 Dec. 1983. Preprint UCRL–90456, Lawrence Livermore National Laboratory, 22 Feb. 1984.
[2] A. Mainomi, 'Proc. 20th Intersociety Energy Conversion Engineering Conference', Miami Beach, FL, August 1985, pp. 2.14–2.20.
[3] A. Despic, *J. Appl. Electrochem.* **15** (1985) 191.
[4] L. A. Knerr, J. C. Huang, D. J. Wheeler and L. J. Gestaut, 'Electrochemical Society Extended Abstracts', New Orleans, LA, 7–12 Oct. 1984, Vol. 84–2, Abstract No. 572, p. 855.
[5] J. Newman, 'Electrochemical Systems', Prentice-Hall, Englewood Cliffs, NJ (1973).
[6] C. Wagner, *J. Electrochem. Soc.* **98** (1951) 116.
[7] J. Newman, in 'Electroanalytical Chemistry' (edited by A. J. Bard), Marcel Dekker, NY (1973) Vol. 6.
[8] G. A. Prentice and C. W. Tobias, *J. Electrochem. Soc.* **129** (1982) 72.
[9] B. Cahan, D. Scherson and M. Reid, *J. Electrochem. Soc.* **00** (1988) 000.
[10] B. Carnahan, H. A. Luther and J. O. Wilke, 'Applied Numerical Methods', John Wiley, NY (1969).
[11] S. L. Gupta, D. Tryk, D. Scherson, W. Aldred and E. Yeager, 'Extended Abstracts of The Electrochemical Society', The Electrochemical Society, Princeton, NJ (1985) Vol. 85–2, Abstract No. 3, pp. 5–6.
[12] U.S. Department of Energy Contract No. 1806205 performed by ELTECH Systems Corporation and administered by the Lawrence Livermore National Laboratory, 1983–1986.
[13] R. E. Carbonio, D. Tryk and E. Yeager, in 'Proc. of Symp. on Electrode Materials and Processes for Energy Conversion and Storage' (edited by S. Srinivasan, S. Wagner and H. Wroblowa), The Electrochemical Society, Pennington, NJ (1987) Vol. 87–12, pp. 238–255.